ADVANCED MATERIALS
www.advmat.de

Mechanochemical Degradation of Poly(vinyl chloride) into Nontoxic Water-Soluble Products via Sequential Dechlorination, Heterolytic Oxirane Ring-Opening, and Hydrolysis

*Neha Choudhury, Ahyun Kim, Minseong Kim, and Byeong-Su Kim**

As one of the most widely used commodity plastics, poly(vinyl chloride) (PVC) is extensively used worldwide, yet is difficult to recycle and is often discarded immediately after use. Its end-of-life treatment often generates toxic hydrogen chloride and dioxins that pose a critical threat to ecosystems. To address this challenge, the mechanochemical degradation of PVC into water-soluble biocompatible products is presented herein. Oxirane mechanophores are strategically introduced into the polymeric backbone via sequential dechlorination followed by epoxidation. The oxirane mechanophore in the polymer backbone undergoes a force-induced heterolytic ring-opening to carbonyl ylide intermediates, which eventually generates acetals during the course of the reaction. The subsequent hydrolysis of the backbone acetals affords the scission of the polymeric chain into water-soluble low-molecular-weight fragments. Combined with its low cytotoxicity and phytotoxicity, this solvent-free mechanochemical degradation process offers a green alternative for the degradation of PVC.

1. Introduction

Plastics have been a staple of modern life since the plastic age began in the 1950s because of their affordability, light weight, and long lifespan.[1,2] They are widely used in a variety of applications, including packaging and consumer products, building and construction, and transportation. Recycling these materials is often challenging due to their durability and chemical stability and as a result, the growing production and use of nonbiodegradable synthetic polymers are placing stress on the environment. A startling 60% of all plastics ever produced ended up in the environment, yet only 9% have been recycled.[3] Both aquatic and terrestrial ecosystems are negatively impacted by the disposal of plastics in coastal areas and downstream waterways and landfills.[4,5] To reduce pollution, it is crucial to rationalize the use of plastic products and raise consumer awareness of the importance of waste recycling and sorting. However, finding practical solutions for processing plastic waste more effectively and, preferably, converting it into biocompatible chemicals is a significant challenge.

Poly(vinyl chloride) (PVC), the third most extensively utilized plastic globally after polyethylene and polypropylene,[6] is a robust and corrosion-resistant material that is frequently used in industries such as construction, transportation, packaging, electrical, and healthcare. Due to these factors, more than 30 million tons of PVC are produced each year worldwide. In contrast to other plastics such as poly(ethylene terephthalate) and polypropylene, PVC is difficult to recycle and is frequently thrown away immediately after use.[7] This generates a large amount of PVC waste,[8] which is frequently disposed of in landfills where additives therein such as potentially carcinogenic phthalates can percolate into the environment.[9] Meanwhile, combusting PVC releases corrosive hydrochloric acid that damages the reactor[10] and toxic dioxins[11] that are harmful to the environment.

Up until now, the dechlorination of PVC has been the primary research focus for attempting to address these issues.[12] Of the several methods for the dechlorination of PVC that have been proposed,[13–15] mechanochemistry has an inevitable place in this list.[16,17] PVC has been successfully dechlorinated by using a planetary ball mill to grind a mixture of PVC and reagents such as sodium hydroxide (NaOH), potassium hydroxide (KOH), and calcium carbonate ($CaCO_3$).[18,19] However, polyenes produced in these reactions are insoluble in the majority of common solvents, which have thus far limited further investigation. Recently, the force-induced mechanochemical activation of mechanophores[20] such as dihalocyclopropanes, oxiranes, spiropyrans, and ladderenes in polymer backbones has attracted significant attention due to its diverse applicability.[21–23] Among them, oxiranes have shown potential as mechanophores that undergo heterolytic ring-opening to generate carbonyl ylides, which facilitate the reaction with surrounding nucleophiles under the influence of extensional shear forces originating from pulsed ultrasound.[24]

N. Choudhury, A. Kim, M. Kim, B.-S. Kim
Department of Chemistry
Yonsei University
Seoul 03722, Republic of Korea
E-mail: bskim19@yonsei.ac.kr

The ORCID identification number(s) for the author(s) of this article can be found under https://doi.org/10.1002/adma.202304113

DOI: 10.1002/adma.202304113

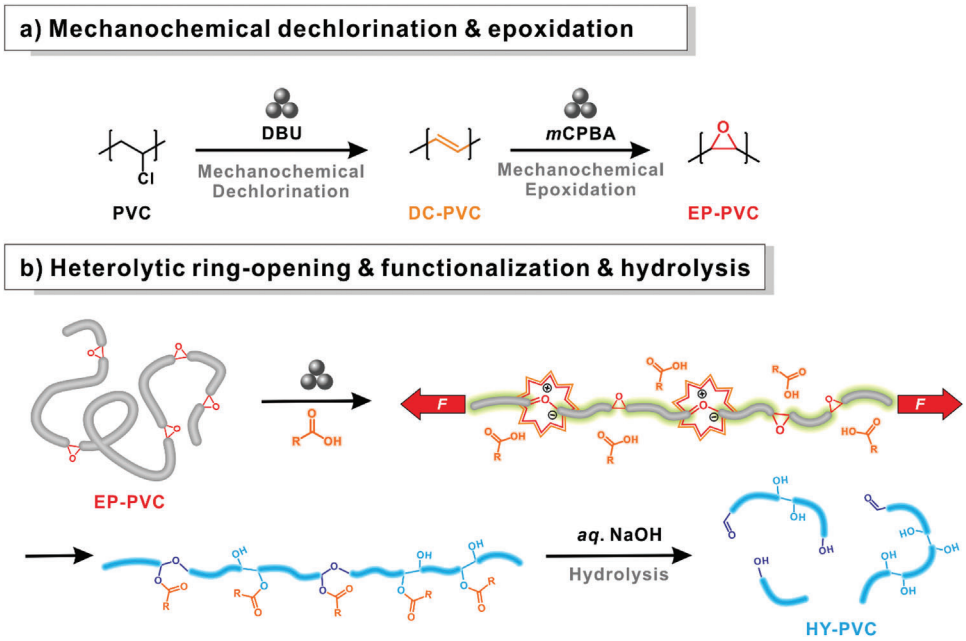

Scheme 1. The mechanochemical degradation of PVC into water-soluble products via sequential dechlorination, epoxidation, and hydrolysis. Note that some functional moieties have been omitted to improve clarity. DC-PVC, dechlorinated PVC; EP-PVC, epoxidized PVC; HY-PVC, hydrolyzed PVC; DBU, 1,8-diazabicyclo[5.4.0]−7-undecene; *m*CPBA, *m*-chloroperoxybenzoic acid.

Inspired by this green solvent-free approach, herein we exploited the heterolytic ring-opening of oxirane mechanophores introduced into the polymeric backbone to degrade the PVC into water-soluble low-molecular-weight products (**Scheme 1**). Specifically, mechanochemical dechlorination followed by epoxidation was applied to install oxirane mechanophores in the polymer backbone. During the course of mechanochemical epoxidation, force-induced heterolytic ring-opening of oxirane mechanophore produced carbonyl ylide intermediates that eventually generated acetals and their ring-opened moieties in the PVC backbone. Subsequent hydrolysis of the backbone acetals afforded the scission of the polymeric chain into water-soluble low-molecular-weight fragments. The practicability of this approach was further demonstrated on commercially available PVC products. We envision that this mechanochemical approach using ball milling offers an excellent means of degrading commodity plastics in a green and solvent-less manner.

2. Results and Discussion

As a starting point for our investigation into PVC degradation, we utilized commercial PVC ($M_{n,GPC}$ = 70.7 kDa) (Figure S1, Supporting Information) as a model substrate (**Figure 1**). The mechanochemical dechlorination of PVC was first optimized by using different types of bases, including NaOH, KOH, $CaCO_3$, and DBU, with a vibrational ball mill (Retsch Mixer Mill MM 400) in a stainless-steel jar with three stainless-steel balls at an operating frequency of 30 Hz. After ball milling, the products from each reaction were rinsed with water and methanol to obtain the dechlorinated PVC (DC-PVC) as a dark brown powder (Figure 1a,b).

Fourier transform infrared (FT-IR) spectroscopy indicated successful dechlorination in all cases with a substantial decrease in absorption peaks at 611 cm^{-1} corresponding to C–Cl stretching in the PVC (Figure 1c and Figure S2, Supporting Information). Moreover, two notable peaks pertaining to C=C stretching at 1688–1527 cm^{-1} and hydroxyl group stretching at 3380 cm^{-1} were observed in the DC-PVC obtained by treatment with all the bases used except for $CaCO_3$. The hydroxyl peaks could have been generated as a result of the reaction between water captured by PVC due to its hygroscopic nature and the C–Cl group of PVC during the ball-milling process via S_N1 reaction under ambient conditions. The degree of dechlorination was calculated by integrating the peak area of C–Cl stretching in DC-PVC referenced to that of pristine PVC (see the Experimental Section for details). It was found that the DBU base provided nearly complete dechlorination compared to the other inorganic bases (Figure 1b). It is noteworthy that structural changes were not evident in a control ball-milling experiment with pristine PVC in the absence of a base, thereby revealing the critical role of the base in the mechanochemical dechlorination process (Figure S3, Supporting Information).

We carefully scrutinized the influence of various mechanochemical parameters on the degree of dechlorination to produce DC-PVC, including the number and size of the milling balls, milling time, and the equivalency of DBU. As expected, the degree of dechlorination became higher as these mechanochemical parameters were increased, which clearly demonstrated that mechanochemical dechlorination was indeed affected by the mechanical force and could be precisely tuned by varying the mechanochemical parameters (Figure 1b; Figures S4, S5, and S6, Supporting Information). In short, nearly complete dechlorination was attained by using three 12 mm-diameter

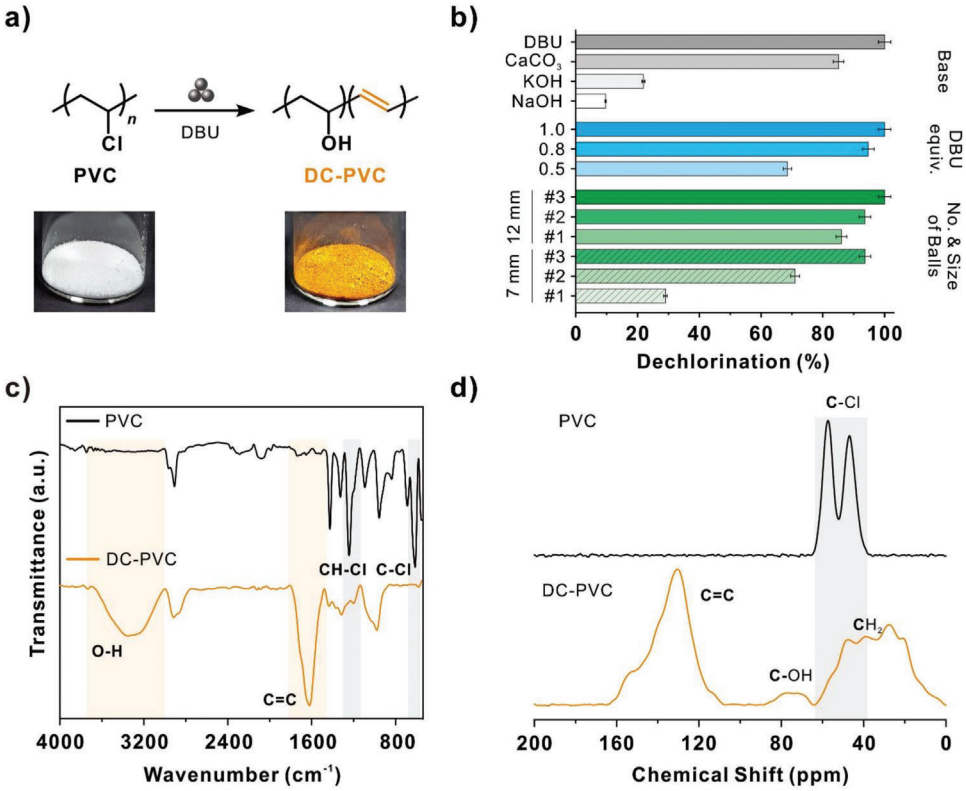

Figure 1. a) Dechlorination of PVC to DC-PVC via the mechanochemical reaction with DBU with a corresponding image of each sample. b) Optimization of the ball-milling conditions for the dechlorination of PVC by FT-IR spectroscopy. c) FT-IR and d) solid-state cross-polarization magic-angle-spinning (CP-MAS) ^{13}C NMR spectra of PVC and DC-PVC obtained under the optimized reaction conditions.

stainless-steel balls, 1.0 equivalence of DBU, and a milling time of 3 h (Figure 1b,c; Figures S5 and S7, Supporting Information).

To verify the results of the FT-IR analysis, DC-PVC was subjected to scanning electron microscopy–energy-dispersive X-ray (SEM-EDX) analysis, the results of which indicate a significant drop in Cl residue in DC-PVC with the degree of dechlorination being 83% (Figure S8, Supporting Information). Since the degree of dechlorination determined by the two analyses was different, X-ray photoelectron spectroscopy (XPS) was performed to further investigate and potentially reconcile these discrepancies. According to XPS measurements, there was an abrupt drop in the atomic percentage of Cl from 7.1% in PVC to 1.2% in DC-PVC, equating to 83% of dechlorination in consistent with the SEX-EDX result (Figure S9, Supporting Information).

To comprehend the thermal stability and decomposition behavior of PVC and DC-PVC, thermogravimetric analysis (TGA) was performed (Figure S10, Supporting Information). PVC powder was found to be thermally stable up to 230 °C, after which rapid dehydrochlorination occurred in the temperature range of 230–380 °C. As the temperature increased to 380–520 °C, the remaining polyene-type molecules were converted into polycondensed aromatic hydrocarbons and eventually into infusible coke with a carbon content of ≈13% after heat treatment up to 900 °C. On the other hand, DC-PVC initially exhibited 4.5% weight loss around 100 °C, attributed to the evaporation of moisture present in the sample (Figure S10, Supporting Information). Subsequently, DC-PVC undergoes thermal decomposition starting from 140 °C, with the polyene structure gradually losing weight as the temperature increases up to 525 °C. After undergoing heat treatment up to 900 °C, the DC-PVC was found to have a fixed carbon yield of 40 wt%. Furthermore, differential scanning calorimetry (DSC) analysis indicated that PVC displayed a glass transition temperature (T_g) at 83.6 °C due to its amorphous nature (Figure S11, Supporting Information). In contrast, DC-PVC exhibited a higher T_g around 154.2 °C ascribed to the polyene structure obtained after dechlorination. A 10.7% weight loss was observed in the DSC thermogram of DC-PVC around 100 °C during the first heating cycle, which could be attributed to the evaporation of water captured by the sample (Figure S11, Supporting Information).

Because DC-PVC is insoluble in common solvents, solid-state cross-polarization magic-angle-spinning (CP-MAS) ^{13}C-NMR spectroscopy was employed to elucidate its structure; the spectrum of pure PVC shows two peaks at 57.4 and 46.8 ppm corresponding to the –C–Cl and –CH_2– groups, respectively. After dechlorination, two new peaks were generated in the region of 160–110 and 90–60 ppm that were attributed to the –C═C– and –C–OH groups, respectively, which is in good agreement with the FT-IR results (Figure 1d).

In the next step, DC-PVC was subjected to in situ mechanochemical epoxidation for the insertion of multiple oxirane mechanophores in the alkene moieties within the polymer backbone (Scheme 1). In situ epoxidation was aimed to induce subsequent heterolytic oxirane ring-opening to generate

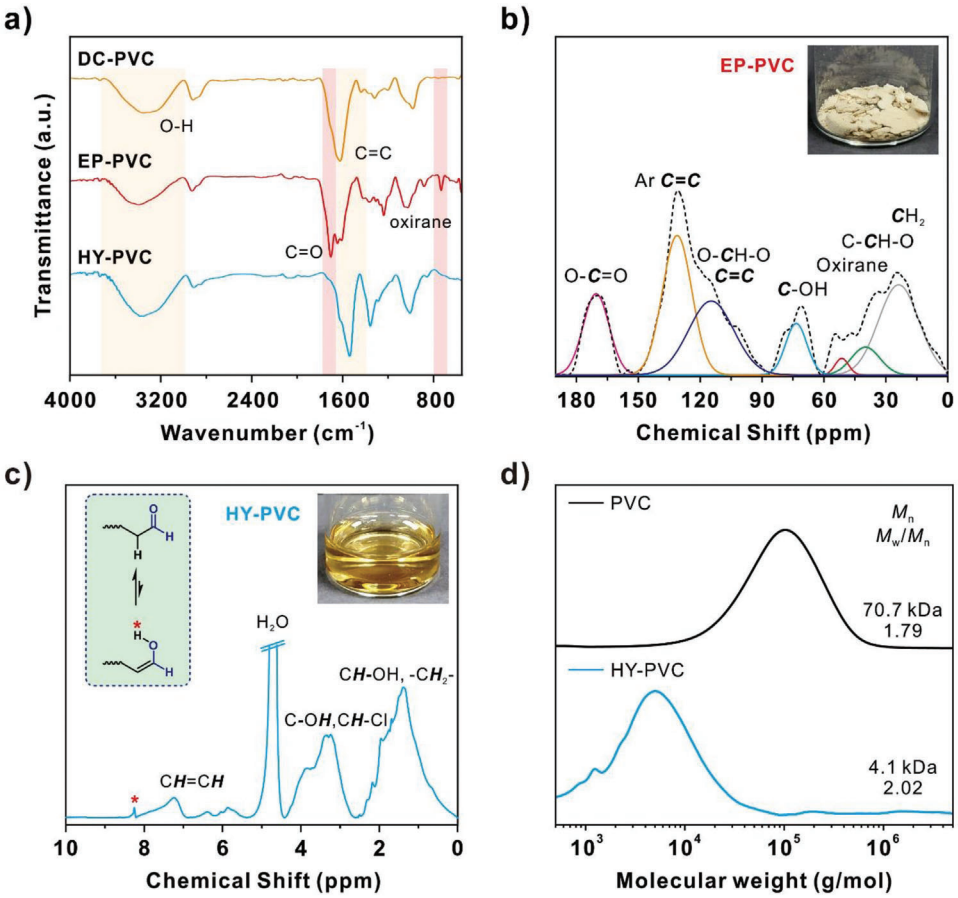

Figure 2. a) FT-IR spectra of DC-PVC, EP-PVC, and HY-PVC produced under optimized ball milling and hydrolysis conditions. b) Deconvoluted high-resolution solid-state CP-MAS ^{13}C NMR spectrum of EP-PVC. c) ^{1}H NMR spectrum of HY-PVC. Inset represents the presence of an enol proton marked with an asterisk. Insets in (b) and (c) are corresponding images of EP-PVC and HY-PVC, respectively. d) Representative gel permeation chromatography (GPC) elugrams of PVC and HY-PVC using THF and water with 0.2 M $NaNO_3$ and 0.01 M NaH_2PO_4 as the eluents, respectively.

carbonyl ylides that subsequently react with the nucleophiles generated during the course of the reaction. DC-PVC was ball milled with several epoxidizing agents such as *m*-chloroperoxybenzoic acid (*m*CPBA), hydrogen peroxide, and *t*-butyl hydroperoxide. Upon completion, the product was washed with methanol and dichloromethane to obtain the epoxidized PVC (i.e., EP-PVC) as an off-white solid (**Figure 2**b).

The FT-IR spectrum of EP-PVC reveals that *m*CPBA yields the highest peak intensities at 897 and 1710 cm^{-1} associated with the stretching frequencies of the oxirane ring and carbonyl group, respectively (Figure S12, Supporting Information). This may propose an involvement of residual *m*-chlorobenzoic acid as a nucleophile that reacted with the epoxide groups formed during the reaction, thereby causing oxirane ring-opening. As a result, *m*-chlorobenzoate groups were incorporated into the polymer backbone, as evidenced by the presence of the carbonyl peak in the FT-IR spectra. Moreover, the intensity of the carbonyl stretching peak was considerably increased by augmenting the amount of *m*CPBA, the milling time, and the number and size of the milling balls (Figures S13–S15, Supporting Information). Maximum epoxidation was achieved using 1.0 equiv of *m*CPBA (with respect to one alkene moiety), three 12 mm stainless-steel balls, and a milling time of 3 h (Figure 2a; Figure S14, Supporting Information). To highlight the advantages of solid-state mechanochemical epoxidation over the solution-phase reaction, DC-PVC was treated with 1 equiv of *m*CPBA in methanol. Interestingly, the extent of epoxidation was less in the solution state compared to 3 h of ball milling even after allowing the reaction to progress for 24 h, thus suggesting the superiority of the latter (Figure S17, Supporting Information). As the temperature inside the milling jar after the mechanochemical epoxidation of DC-PVC with *m*CPBA increased to 52.5 °C (Figure S16, Supporting Information), another solution-state epoxidation was carried out at 55 °C. The extent of epoxidation was still significantly lower compared to 3 h of the ball-milling process (Figure S17, Supporting Information).

CP-MAS ^{13}C-NMR spectroscopy provided meaningful insight into the mechanistic possibilities of simplifying the structure of EP-PVC (Figure 2b). While the exact chemical structure of EP-PVC is still elusive, the appearance of a new peak in the region of 183–158 ppm specified the existence of the ester carbonyl group. Moreover, the increased peak areas in the ranges of 150–88 ppm and 86–60 ppm suggest the formation of aromatic C=C groups in the polymeric chain and new C–OH groups during the course of the reaction. The increase in atomic percentage of Cl from 1.2% in DC-PVC to 1.8% in EP-PVC further suggested the

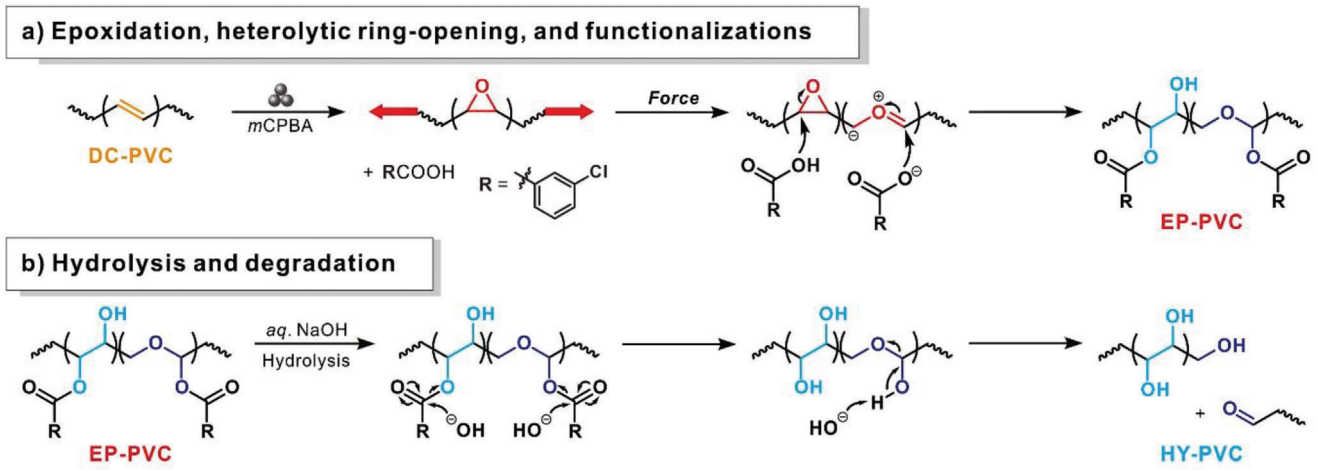

Figure 3. The proposed stepwise mechanism during the mechanochemical degradation of PVC into water-soluble HY-PVC products.

incorporation of *m*-chlorobenzoate groups into the polymeric pendant (Figure S9, Supporting Information).

On the basis of the FT-IR and ^{13}C-NMR analyses, we can deduce the following plausible mechanistic processes (**Figure 3**a). 1) Initially, several oxirane moieties are generated via the reaction between the alkene moieties present in the polymeric backbone of DC-PVC and *m*CPBA following the conventional epoxidation reaction. 2) Interaction between the oxirane groups and *m*-chlorobenzoic acid formed during the reaction leads to oxirane ring-opening, resulting in the generation of hydroxyl groups and insertion of *m*-chlorobenzoate groups in the polymeric pendant. 3) Most notably, under mechanochemical conditions, some of the oxirane moiety behaves as a mechanophore undergoing force-induced ring-opening to provide carbonyl ylide intermediates, which can then react with *m*-chlorobenzoic acid to form acetals.

To validate the acetal generation in the preceding stage, we performed the hydrolysis of EP-PVC to afford water-soluble hydrolyzed HY-PVC (Figure 2c inset). While both acids and bases can catalyze the hydrolysis of EP-PVC, aqueous NaOH required only 30 min to complete the reaction, whereas HCl took around 12 h and required the time-consuming removal of excess HCl from the product. Hence, because both reaction routes provided nondistinguishable products, as confirmed via FT-IR spectroscopy (Figure 2a; Figure S18, Supporting Information), we prioritized base hydrolysis in this study. For example, carbonyl stretching at 1710 cm^{-1} vanished completely while the peak intensity of hydroxyl stretching at 3376 cm^{-1} rose, thereby indicating successful hydrolysis of the ester upon treatment with a base (Figure 2a). Moreover, examination of the ^{1}H NMR spectrum of HY-PVC revealed a peak at 8.24 ppm ascribed to the proton of the enol tautomer of aldehyde in water (Figure 2c).[25] In addition, the vinylic protons (both conjugated and nonconjugated) were present in the polymer backbone, as evidenced by the proton peaks in the range of 7.89–5.45 ppm. Based on the aforementioned findings, we propose the following mechanism for the base-catalyzed hydrolysis of EP-PVC to HY-PVC (Figure 3b). Specifically, typical ester hydrolysis initially takes place to produce hemiacetals, which in turn, react under basic conditions to generate the aldehyde[26] and, most importantly, degrade the polymeric backbone into smaller fragments. The isolated yield of HY-PVC obtained from powder PVC is around 60%. Gel permeation chromatography (GPC) analysis indicates that the molecular weight of HY-PVC is 4.1 kDa, which is nearly 17-fold smaller than the initial molecular weight of PVC (70.7 kDa) (Figure 2d).

In clear contrast, the control sample of the epoxidized PVC obtained from solution-state epoxidations of DC-PVC did not result in any water-soluble product. FT-IR spectroscopy of the products revealed the absence of carbonyl stretching at 1710 cm^{-1} and an increase in the peak intensity of hydroxyl stretching at 3376 cm^{-1} (Figure S19, Supporting Information). The insolubility of the products in water implied that the polymeric chain was not degraded in lower-molecular-weighted fragments during hydrolysis, further supporting the mechanistic insight of our mechanochemical approach.

Since our main objective was to degrade PVC into nontoxic biocompatible products, the biocompatibility of HY-PVC was assessed by 3-(4,5-dimethylthiazol-2-yl)-2,5-diphenyltetrazolium bromide (MTT)-based cytotoxicity assay utilizing mouse fibroblast L929 cell line. Even at the high HY-PVC concentration of 500 μg mL^{-1}, the cell viability remained greater than 80%, inferring reasonable biocompatibility (**Figure 4**a). Furthermore, we investigated the phytotoxicity of HY-PVC on the germination rate of *Lactuca sativa* L. (lettuce) seeds treated with various concentrations of HY-PVC.[27] After incubating for 5 days at 25°C in 75% relative humidity, the relative root lengths were assessed (Figure 4b; Figure S20, Supporting Information), the results of which indicate a germination rate greater than 50% after treatment with up to 8 mg mL^{-1} of HY-PVC. The acceptable biocompatibility and low phytotoxicity of HY-PVC highlight the efficacy of this green route for dealing with PVC waste.

The practical applicability of our protocol was further validated to degrade various commercially available PVC products (Figure 4c; Figures S21–S23, Supporting Information). At first, the PVC products with different mechanical strengths were chopped into small pieces (PVC_H: 5 mm × 3 mm; PVC_M: 5 mm × 4 mm; and PVC_S: 4 mm × 4 mm) and subjected to mechanochemical dechlorination with DBU (Figure 4c; Figures

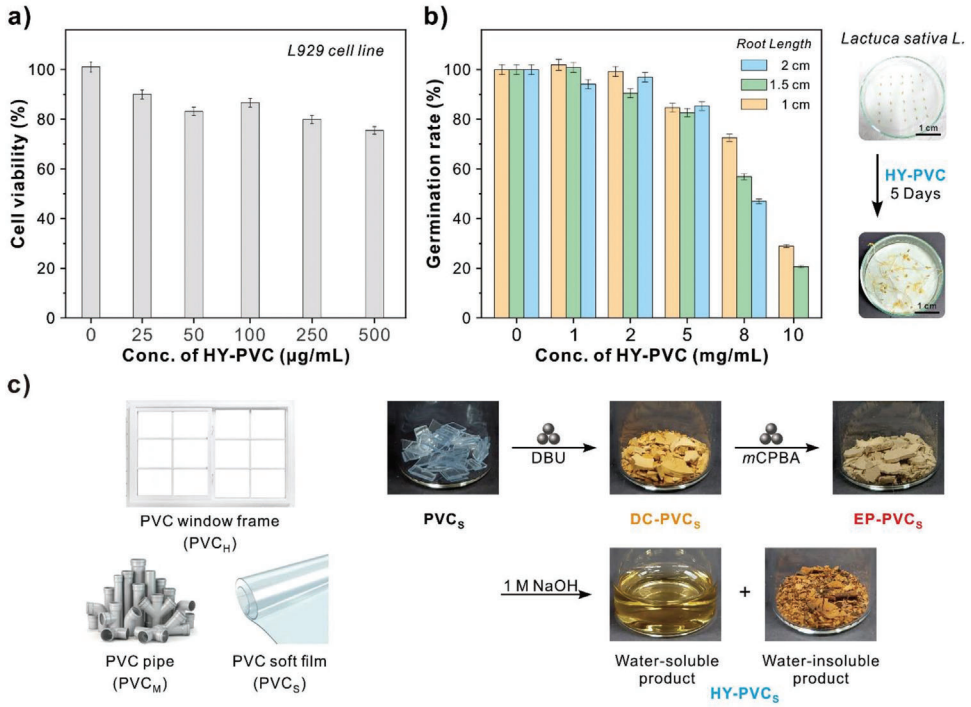

Figure 4. a) MTT cytotoxicity assay of HY-PVC using L929 cell line. b) The germination rate of *Lactuca sativa* L. seeds after treatment with various concentrations of HY-PVC with respect to the root length of the germinated seeds after 5 days of growth with corresponding images of the germinated seeds after treatment with 5 mg mL^{-1} of HY-PVC (scale bar: 1 cm). c) Images of commercially available PVC products (left) and the products obtained after treatment via our protocol (right). PVC$_H$, window frame; PVC$_M$, hard film; PVC$_S$, soft film. Subscripts H, M, and S stand for hard, moderately hard, and soft, respectively. Note that the commercial PVC product resulted in both water-soluble and water-insoluble products unlike PVC powder.

S22 and S23, Supporting Information). The appearance of C=C stretching at 1688–1520 cm^{-1} and the reduction of the C–Cl stretching peak at 611 cm^{-1} in the FT-IR spectra indicate the successful dechlorination of the PVC in all three cases (Figures S21–S23, Supporting Information). In the subsequent step, the presence of the C=O stretching peak at 1710 cm^{-1} served to corroborate successful mechanochemical epoxidation (Figures S21–S23, Supporting Information). Finally, treatment with a base yielded two types of products: water-soluble and water-insoluble ones, unlike the previous PVC powder sample. The relative amount of each product of HY-PVCs obtained from different EP-PVCs are listed in Table S1 (Supporting Information). According to the FT-IR spectra, both products possessed similar functional groups in the polymeric chain (Figures S21–S23, Supporting Information). The ^{1}H NMR spectra of water-soluble HY-PVCs were nearly identical to that of HY-PVC obtained from PVC powder (Figure S24, Supporting Information); however, some sharp aromatic proton peaks in the range of 7.8–7.3 ppm were observed, which could be due to the presence of aromatic plasticizers or stabilizers in the commercial PVCs. The elemental analysis revealed that the weight percentage of carbon in water-insoluble HY-PVC$_S$ was substantially high (46.0%) compared to water-soluble HY-PVC$_S$ (34.7%) (Table S2, Supporting Information), whereas the weight percentage of oxygen is in the reverse order (34.8% in water-insoluble HY-PVC$_S$ and 39.9% water-soluble HY-PVC$_S$), possibly explaining the insolubility of the former. Additionally, according to CP-MAS ^{13}C-NMR spectroscopy, water-soluble HY-PVC$_S$ displayed a higher content of C–OH moiety compared to water-insoluble HY-PVC$_S$ consistent with the elemental analysis result (Figure S25, Supporting Information). When compared to PVC and DC-PVC, the water-insoluble part of HY-PVC is also considered to be significantly more environmentally benign owing to the presence of high fraction of hydroxyl group without Cl residue.

To further provide evidence of our degradation mechanism, the molecular weight of the degraded water-soluble HY-PVC was characterized via GPC analysis: the $M_{n,GPC}$ values were 3.6, 2.7, and 2.8 kDa for the PVC from the soft film, hard film, and window frame, respectively (Figure S26, Supporting Information). In addition, the effect of the size of commercial PVC pieces on the amount of water-soluble and insoluble HY-PVC was studied using PVC$_S$ as an example. Beside the original PVC$_S$ sample (4 mm × 4 mm), two PVC$_S$ samples of different sizes (PVC$_{S1}$: 2 mm × 2 mm and PVC$_{S2}$: 8 mm × 8 mm) were prepared and subjected to consecutive mechanochemical dechlorination, epoxidation, and hydrolysis under optimized conditions. The products isolated in each step were characterized by FT-IR spectroscopy (Figures S27 and S28, Supporting Information). Intriguingly, the reduction of the size of the PVC$_S$ resulted in a significant increase in the amount of water-soluble HY-PVC$_{S1}$ (220 mg) compared to that from the original HY-PVC$_S$ (70 mg) (Table S3, Supporting Information). This observation could imply that reducing the size of PVC enhanced the surface area-to-volume ratio of the particles, which promoted the efficiency under ball-milling conditions. It is evident from the results above that our technique is effective at degrading

a variety of PVC products of varying grades and molecular weights, while there are still room for further optimization to tailor the outcome of the reactions.

3. Conclusions

Mechanochemical ball milling was applied to degrade PVC into nontoxic water-soluble products. Our process involving solid-state mechanochemical dechlorination and epoxidation offers a green alternative to the conventional solution-based reaction process. The most significant effect of the ball-milling process was force-induced heterolytic oxirane ring-opening that aids PVC degradation into smaller fragments. Our strategy utilized only three relatively nonhazardous chemicals–DBU, *m*CPBA, and NaOH–to convert PVC into water-soluble HY-PVC. To date, several catalytic and biodegradation processes were reported to degrade commodity polymers like polyester, polyolefin (HDPE and LDPE), PVC, and PS. The cost of catalysts, enzymes, or other degrading agents, as well as the infrastructure needed to deploy them, can be prohibitively expensive. Scaling up these systems to handle large amounts of plastic garbage may necessitate huge investments as well. However, our approach does not require any sophisticated instrumentation or expensive chemicals and the reaction can be readily scaled up from the laboratory scale to industrial scale. Thus, it has the advantages of being economical and environmentally friendly compared to existing degradation techniques. In addition, the relatively good biocompatibility with low phytotoxicity of the HY-PVC product makes our approach relatively harmless to both aquatic and terrestrial ecosystems. Notably, several commercial PVC products were degraded using our methodology, suggesting that the solid-state mechanochemical approach could be used to degrade other commodity polymers without the need for extensive chemical reactions and expensive catalysts. We thus anticipate that the approach suggested in this study will stimulate the development of new direction for degrading petroleum-based nondegradable commodity plastics.

4. Experimental Section

Materials: Poly(vinyl chloride) (PVC; molecular weight: 48 000 g mol^{-1}), *m*-chloroperoxybenzoic acid (*m*CPBA), and calcium carbonate ($CaCO_3$) were purchased from Sigma-Aldrich. 1,8-Diazabicyclo[5.4.0]−7-undecene (DBU) and hydrogen peroxide (H_2O_2) were obtained from TCI Sejin Cl. Sodium hydroxide (NaOH) beads and potassium hydroxide (KOH) flakes were acquired from Duksan and Daejung Chemicals, respectively. *tert*-Butyl hydroperoxide (*t*BuOOH) was purchased from Alfa-Aesar. A dialysis membrane (Spectra/Por6 MWCO-1 kDa; flat width: 38 mm and diameter: 24 mm) was purchased from Spectrum Laboratories, USA. Dichloromethane (DCM) and methanol (MeOH) were purchased from SK Chemicals. Deuterated NMR solvent deuterium oxide (D_2O) was purchased from Cambridge Isotope Laboratory. All chemicals were of analytical grade and used without further purification unless otherwise indicated. Three different types of commercially available PVC products: window frame, hard film, and soft film denoted as PVC_H, PVC_M, and PVC_S, respectively (subscripts H, M, and S stand for hard, moderately hard, and soft, respectively), were purchased from coupang.com, a South Korea e-commerce company.

Characterization: The ball-milling experiments were carried out in a Retsch Mixer Mill MM 400 with a 25 mL stainless-steel jar and stainless-steel balls (7 or 12 mm in diameter). An FT-IR spectrophotometer (Cary 630, Agilent) equipped with an attenuated total reflection (ATR) module was utilized to obtain FT-IR spectra. Solid-state cross-polarization magic-angle-spinning (CP-MAS) ^{13}C-NMR spectra were recorded with a Bruker AVANCE II+ 400-MHz NMR system at a frequency of 12 kHz and 30 s delay time at the Korea Basic Science Institute (KBSI) Seoul Western Center. A field emission-scanning electron microscope (FE-SEM) (JEOL-7800F) at an accelerating voltage of 10 kV was used to obtain scanning electron microscopy–energy-dispersive X-ray (SEM-EDX) images of C-Cl residues in samples. The molecular weight and dispersity (*Đ*) of PVC was measured by utilizing a gel permeation chromatography (GPC) apparatus (Agilent 1200 series) with a refractive index (RI) detector at room temperature. The sample was eluted at a flow rate of 1.0 mL min^{-1} with tetrahydrofuran (THF). Poly(methyl methacrylate) (PMMA) was used as a standard to calibrate the instrument. The molecular weight and dispersity (*Đ*) of a variety of hydrolyzed poly(vinyl chloride) (HY-PVC) were measured by utilizing another GPC apparatus (Agilent 1260 Infinity system) with an RI detector using PL aquagel-OH MIXED-M 8 µm columns at room temperature. Samples were eluted at a flow rate of 1.0 mL min^{-1} with aqueous solutions of 0.2 M sodium nitrate ($NaNO_3$) and 0.01 M sodium dihydrogen phosphate (NaH_2PO_4). Poly(ethylene glycol) (PEG) standards were used to calibrate the instrument. ^{1}H NMR spectra were recorded at 25 °C on a Bruker 400 MHz spectrometer. Freeze dryer TFD8501 was used to lyophilize the samples. Thermogravimetric analysis (TGA) was performed using a TGA Q50 analyzer (TA instruments). Differential scanning calorimetry (DSC) was carried out utilizing a Q200 model (TA Instruments) between −80 and 200 °C at a heating and cooling rate of 10 °C min^{-1} under a nitrogen (N_2) atmosphere. X-ray photoelectron spectroscopy (XPS) was performed using K-alpha (Thermo Scientific Inc., UK). An elemental analyzer (Thermo Scientific FLASH 2000) was utilized for elemental analysis.

Mechanochemical Dechlorination of PVC: PVC (0.50 g) and DBU (1 equiv with respect to one monomeric unit) were added to a 25 mL stainless-steel milling vial equipped with three stainless-steel milling balls (12 mm in diameter). The tightly sealed vial was placed in a vibrational ball mill (Retsch Mixer Mill MM 400) and subjected to milling for 3 h at 30 Hz. The milling vial was then opened, and the product was washed with water and MeOH, respectively. Finally, the product was dried at room temperature for 24 h to obtain the dechlorinated PVC (DC-PVC) as a dark brown powder with an isolated yield of 86%. Before performing the thermal analysis, DC-PVC was vacuum dried at 60 °C for 12 h, after then, azeotropic distillation was additionally conducted on DC-PVC to eliminate any residual water.

Calculation of Degree of Dechlorination: The degree of dechlorination of different DC-PVCs was calculated by integrating the peak area of C-Cl stretching at 611 cm^{-1} in DC-PVCs with reference to pristine PVC

$$\text{Degree of Dechlorination} = \left[\frac{(\text{Peak area for C–Cl in PVC}) - (\text{Peak area for C–Cl in DC-PVC})}{\text{Peak area for C} - -\text{Cl in PVC}}\right] \times 100\% \quad (1)$$

Mechanochemical Epoxidation of DC-PVC: To a 25 mL of stainless-steel milling vial, DC-PVC (200 mg) and *m*CPBA (1 equiv with respect to one alkene moiety) were added with three stainless-steel milling balls (12 mm in diameter). The tightly sealed vial was then secured in a vibrational ball mill (Retsch Mixer Mill MM 400) and milled at 30 Hz for 3 h. Finally, the product was sequentially washed with MeOH and DCM and dried at room temperature for 24 h to obtain the epoxidized PVC (EP-PVC) as an off-white solid with an isolated yield of 83%.

Solution-State Epoxidation of DC-PVC: DC-PVC (200 mg) and *m*CPBA (1 equiv with respect to one alkene moiety) were placed in a 50 mL round-bottomed flask along with 6 mL of methanol. The reaction mixture was stirred for 24 h at room temperature (or 55 °C). Finally, the product was washed with MeOH and DCM and dried at room temperature for 24 h to obtain the epoxidized PVC as a pale-yellow solid with an isolated yield of ≈90%.

Hydrolysis of EP-PVC to HY-PVC under Basic Conditions: In a 10 mL glass vial, 500 mg EP-PVC was placed with a magnetic stir bar. Subsequently, 6 mL of 1 M NaOH solution was added, and the mixture was stirred vigorously for 30 min, after which the powder was completely

soluble in water. To remove excess NaOH, the solution was dialyzed in water for 12 h using a dialysis membrane with MWCO-1 kDa. Finally, the dialyzed solution was lyophilized, yielding HY-PVC as a light brown fiber-like solid with an isolated yield of 80%.

In Vitro Cell Viability Assay: The viability of mouse fibroblast cells (the L929 cell line) was quantified by the 3-(4,5-dimethylthiazol-2-yl)-2,5-diphenyltetrazolium bromide (MTT)-based cytotoxicity assay. Initially, L929 cells were grown in RPMI-1640 (with L-glutamine) containing 10% fetal bovine serum (FBS) and 1% antibiotic–antimycotic (penicillin–streptomycin 10 000 U mL^{-1}). The cells were cultured in a humidified incubator at 37 °C with 5% CO_2 for 48 h. The cells were then seeded in a 96-well plate at a concentration of 1.5×10^5 cells per mL and incubated for 24 h. Subsequently, the cells were exposed to the HY-PVC sample at various concentrations (0, 25, 50, 100, 250, and 500 µg mL^{-1}) and incubated for an additional 24 h at 37 °C under 5% CO_2. The cells were then washed twice with phosphate-buffered saline (PBS, pH 7.4) before being incubated for 4 h at 37 °C with 100 µL of MTT solution. After dissolving the resultant formazan crystals in dimethyl sulfoxide (DMSO) for 30 min, the absorbance was measured at 570 nm by using a microplate reader (Perkin Elmer VICTOR X5). The results were then compared to those from the control experiment.

Seed Germination Assay: *Lactuca sativa* L. (lettuce) seeds were used to investigate the phytotoxicity of HY-PVC. Prior to testing, the seeds were sequentially washed three times with 3% H_2O_2 and distilled water. Solutions of HY-PVC at various concentrations (0–10 mg mL^{-1}) in a total volume of 5 mL of distilled water were then placed in a Petri dish with a clean piece of Whatman No. 2 filter paper. Next, 30 seeds were scattered over the filter paper, after which the Petri dish was covered with a lid and incubated for five days at 25 °C under 75% relative humidity. Finally, the root lengths of the germinated seeds were measured, and the germination rates were computed as follows:

$$\text{Germination rate}\,(\%) = \left(\frac{\text{Number of germinated seeds}}{\text{Total number of seeds}}\right) \times 100\% \qquad (2)$$

Supporting Information

Supporting Information is available from the Wiley Online Library or from the author.

Acknowledgements

This work was supported by the National Research Foundation of Korea (NRF-2021R1A2C3004978 and NRF-2018R1A5A1025208) and the Samsung Research Funding & Incubation Center of Samsung Electronics under Project Number SRFC-MA1902-05. The authors appreciate Prof. Jeyoung Park in Sogang University for his guidance in phytotoxicity assay.

Conflict of Interest

The authors declare no conflict of interest.

Data Availability Statement

The data that support the findings of this study are available from the corresponding author upon reasonable request.

Keywords

heterolytic oxirane ring-opening, hydrolysis, mechanochemical reaction, PVC degradation

Received: May 3, 2023
Revised: June 19, 2023
Published online:

[1] R. C. Thompson, S. H. Swan, C. J. Moore, F. S. vom Saal, *Philos. Trans. R. Soc. B: Biol. Sci.* **2009**, *364*, 1973.
[2] J. Hopewell, R. Dvorak, E. Kosior, *Philos. Trans. R. Soc. B: Biol. Sci.* **2009**, *364*, 2115.
[3] R. Geyer, J. R. Jambeck, K. L. Law, *Sci. Adv.* **2017**, *3*, e1700782.
[4] M. A. Browne, P. Crump, S. J. Niven, E. Teuten, A. Tonkin, T. Galloway, R. Thompson, *Environ. Sci. Technol.* **2011**, *45*, 9175.
[5] J. R. Jambeck, R. Geyer, C. Wilcox, T. R. Siegler, M. Perryman, A. Andrady, R. Narayan, K. L. Law, *Science* **2015**, *347*, 768.
[6] L. Ye, C. Qi, J. Hong, X. Ma, *J. Clean Prod.* **2017**, *142*, 2965.
[7] K. Ragaert, L. Delva, K. Van Geem, *Waste Manage.* **2017**, *69*, 24.
[8] M. Sadat-Shojai, G.-R. Bakhshandeh, *Polym. Degrad. Stab.* **2011**, *96*, 404.
[9] H. M. Koch, H. Drexler, J. Angerer, *Int. J. Hyg. Environ. Health* **2003**, *206*, 77.
[10] A. Buekens, K. Cen, *J. Mater. Cycles Waste Manag.* **2011**, *13*, 190.
[11] M. Y. Wey, K. Y. Liu, W. J. Yu, C. L. Lin, F. Y. Chang, *Waste Manage.* **2008**, *28*, 406.
[12] G. Grause, A. Buekens, Y. Sakata, A. Okuwaki, T. Yoshioka, *J. Mater. Cycles Waste Manag.* **2011**, *13*, 265.
[13] M. A. Keane, *J. Chem. Technol. Biotechnol.* **2007**, *82*, 787.
[14] S. Moulay, *Prog. Polym. Sci.* **2010**, *35*, 303.
[15] J. Yu, L. Sun, C. Ma, Y. Qiao, H. Yao, *Waste Manage.* **2016**, *48*, 300.
[16] G. Cagnetta, J. Robertson, J. Huang, K. Zhang, G. Yu, *J. Hazard. Mater.* **2016**, *313*, 85.
[17] G. Cagnetta, K. Zhang, Q. Zhang, J. Huang, G. Yu, *Waste Manage.* **2018**, *75*, 181.
[18] T. Inoue, M. Miyazaki, M. Kamitani, J. Kano, F. Saito, *Adv. Powder Technol.* **2005**, *16*, 27.
[19] M. Baláž, Z. Bujňáková, M. Achimovičová, M. Tešinský, P. Baláž, *Environ. Res.* **2019**, *170*, 332.
[20] R. T. O'Neill, R. Boulatov, *Nat. Rev. Chem.* **2021**, *5*, 148.
[21] M. H. Barbee, J. Wang, T. Kouznetsova, M. Lu, S. L. Craig, *Macromolecules* **2019**, *52*, 6234.
[22] K. Kubota, N. Toyoshima, D. Miura, J. Jiang, S. Maeda, M. Jin, H. Ito, *Angew. Chem., Int. Ed.* **2021**, *60*, 16003.
[23] S. Zhang, L. Han, H. Bai, C. Li, X. Wang, Z. Yang, M. Zai, H. Ma, Y. Li, *ACS Sustainable Chem. Eng.* **2021**, *9*, 8053.
[24] H. M. Klukovich, Z. S. Kean, A. L. B. Ramirez, J. M. Lenhardt, J. Lin, X. Hu, S. L. Craig, *J. Am. Chem. Soc.* **2012**, *134*, 9577.
[25] D. A. Ossipov, K. Bränvall, K. Forsberg-Nilsson, J. Hilborn, *J. Appl. Polym. Sci.* **2007**, *106*, 60.
[26] T. J. Przystas, T. H. Fife, *J. Am. Chem. Soc.* **1981**, *103*, 4884.
[27] S. Ju, G. Shin, M. Lee, J. M. Koo, H. Jeon, Y. S. Ok, D. S. Hwang, S. Y. Hwang, D. X. Oh, J. Park, *Green Chem.* **2021**, *23*, 6953.